THE PROTEIN SOCIETY

Plasticity and transient binding are key ingredients of the periplasmic chaperone network

Aaron P. Chum, Sophie R. Shoemaker, Patrick J. Fleming, and Karen G. Fleming *

T.C. Jenkins Department of Biophysics, Johns Hopkins University, Baltimore, Maryland

Received 31 January 2019; Accepted 6 May 2019
DOI: 10.1002/pro.3641
Published online 23 May 2019 proteinscience.org

Abstract: **SurA, Skp, FkpA, and DegP constitute a chaperone network that ensures biogenesis of outer membrane proteins (OMPs) in Gram-negative bacteria. Both Skp and FkpA are holdases that prevent the self-aggregation of unfolded OMPs, whereas SurA accelerates folding and DegP is a protease. None of these chaperones is essential, and we address here how functional plasticity is manifested in nine known null strains. Using a comprehensive computational model of this network termed OMPBioM, our results suggest that a threshold level of steady state holdase occupancy by chaperones is required, but the cell is agnostic to the specific holdase molecule fulfilling this function. In addition to its foldase activity, SurA moonlights as a holdase when there is no expression of Skp and FkpA. We further interrogate the importance of chaperone–client complex lifetime by conducting simulations using lifetime values for Skp complexes that range in length by six orders of magnitude. This analysis suggests that transient occupancy of durations much shorter than the *Escherichia coli* doubling time is required. We suggest that fleeting chaperone occupancy facilitates rapid sampling of the periplasmic conditions, which ensures that the cell can be adept at responding to environmental changes. Finally, we calculated the network effects of adding multivalency by computing populations that include two Skp trimers per unfolded OMP. We observe only modest perturbations to the system. Overall, this quantitative framework of chaperone–protein interactions in the periplasm demonstrates robust plasticity due to its dynamic binding and unbinding behavior.**

Keywords: membrane protein folding; chaperones; computational modeling; holdase

Introduction

Holdases are ATP-independent chaperones that function through an antiaggregation activity.[1–3] The periplasmic compartment of a Gram-negative bacterium is an ideal cellular location for holdase chaperones to play pivotal roles in proteostasis. In contrast to the cytoplasm, the periplasm is devoid of an external energy source, eliminating the option for ATP-driven chaperones. Some periplasmic activities overcome this energetic limitation by connecting their functions to ATP usage through interactions with inner membrane proteins, but all other processes that are uncoupled from the energized inner membrane must rely on ATP-independent mechanisms for efficient execution. Included in the energy-independent activities essential for life is the biogenesis of outer membrane proteins (OMPs).

The maturation of OMPs *in vivo* is a remarkable feat given their trafficking challenges. OMP polypeptides are translated in the cytoplasm, transported in

Additional Supporting Information may be found in the online version of this article.

Karen G. Fleming: Lead contact

Grant sponsor: Directorate for Biological Sciences MCB1412108; Grant sponsor: National Institute of General Medical Sciences R01GM079440.

*Correspondence to: Karen G. Fleming, T.C. Jenkins Department of Biophysics, Johns Hopkins University, Baltimore, Maryland. E-mail: karen.fleming@jhu.edu

Published by Wiley © 2019 The Protein Society

an unfolded conformation across the bacterial inner (cytoplasmic) membrane, and then are passed through the aqueous compartment of the periplasm to reach their native location for folding, which is the outer membrane. Although energy is consumed during the translocon-mediated export of unfolded OMPs (uOMPs) across the inner membrane, both the periplasmic crossing and the outer membrane folding events must occur in the absence of external energy. Notably, OMPs are insoluble in water in both native and unfolded forms,[4,5] which means that the challenge for the cell is to maintain OMPs in unfolded, yet soluble, folding-competent conformations until they fold into the outer membrane. Given the poor solvent (i.e., water) faced by OMPs in the periplasm, they self-aggregate in aqueous solutions, and therefore it seems only appropriate for holdase chaperones to feature prominently in OMP homeostasis. Four proteins in particular have been identified as general chaperones that ensure efficient OMP biogenesis. Two of these function as holdases, Skp (17-kDA protein)[6–8] and FkpA (FKPB-type peptidyl-prolyl *cis-trans* isomerase FkpA).[9] There are two additional proteins aiding biogenesis: one functions as a foldase to accelerate folding, SurA (survival factor A),[10–12] and the other acts as a periplasmic protease, DegP[13] (periplasmic serine endoprotease DegP).

Paradoxically, genetic studies demonstrate that none of the single gene deletion or depletion strains (Δ*surA*, Δ*skp*, Δ*fkpA*, and Δ*degP*) of these general chaperones is lethal in *Escherichia coli.* Many double null strains are also viable (Δ*surA*Δ*degP*, Δ*skp*Δ*fkpA*, Δ*skp*Δ*degP*, and Δ*surA*Δ*skp*) with the caveat that the Δ*surA*Δ*skp* strain is synthetic lethal in rich media but not minimal media.[14] Altogether, the preponderance of viable phenotypes indicates no single protein in this set is an OMP biogenesis linchpin. Rather, a robust functional redundancy must exist among these chaperones.

To simultaneously consider all chaperone:uOMP binding interactions and their mutual effects, we previously incorporated experimentally available genetic and biophysical findings into a kinetic framework for the periplasm that simultaneously considers all reactions in this process. This computational model of the periplasmic chaperone system—termed "Outer Membrane Protein Biogenesis Model" (OMPBioM)—consists of a series of ordinary differential equations that describes all of the known protein–protein interactions within this periplasmic chaperone network as well as cellular concentrations from proteomics.[15] Figure 1 shows a schematic of this network model. In addition to deterministic calculations using parameters to model exponentially growing cells, we previously conducted stochastic simulations in which each rate constant in the master equation was modified by a probability distribution function to introduce randomness into the system. Demonstrating robustness of the deterministic output, the stochastic simulations found that the system of equations in the computational model successfully reproduces the average copy number for OMPs, the mean periplasmic lifetimes for uOMPs, and phenotypic signatures for single- or double-null strain genotypes, including reduced OMP levels in the outer membrane and increased aggregated protein in the periplasm.

Here, we conduct additional stochastic simulations to evaluate how the chaperone populations work individually and together within this periplasmic network. Our first focus is on SurA:U (1:1 stoichiometric complex between one SurA and one uOMP), Skp_3:U (1:1 stoichiometric complex between one Skp trimer and one uOMP), and $FkpA_2$:U (1:1 stoichiometric complex between one FkpA dimer and one uOMP) population distributions relative to one another in nine distinct null strains. Overall, our results indicate that holdase activity must be present in the periplasm, but the specific chaperone dominating this functional role is not critical as long as free (unbound) uOMPs do not accumulate. We next used OMPBioM to address two novel questions. The first concerns multivalency of Skp_3 interactions with uOMP, in which we model a $2(Skp_3)$:U (2:1 complex between two Skp trimers and one uOMP), which has been observed in mass spectrometry experiments.[16] Our data show that the formation of $2(Skp_3)$:U has only a modest effect on the population distribution and, paradoxically, reduces the activity of Skp_3 toward additional clients. The second new question interrogates conflicting data on the lifetime of Skp_3:U. Published experimental values from different groups for the Skp_3:U complex lifetime vary from milliseconds to hours.[17,18] We conducted a parameter scan over six orders of magnitude of Skp_3:U lifetimes, and our results indicate that the holdase activity of Skp is unlikely to be manifested by Skp trimers "holding on" to uOMP clients for lengthy amounts of time. Rather, transient Skp_3 occupancy by uOMPs appears to be the key holding function, and Skp_3:U complexes are only populated if their formation is characterized by rapid association and dissociation. This characteristic of Skp_3:U complex assembly allows the envelope stress response system to rapidly sense the accumulation of free uOMPs, which are stress signals in the periplasmic space. Mechanistically, dynamic binding and unbinding provides network regulation that allows a facile cellular response to any environmental perturbations.

Results and Discussion

The predominant holdase chaperone is determined by the needs of the strain genotype

We determined species distributions of chaperone:uOMP complexes to ask how the observed genetic redundancy can be so robustly encoded across the nine different (single and double) null strains. For

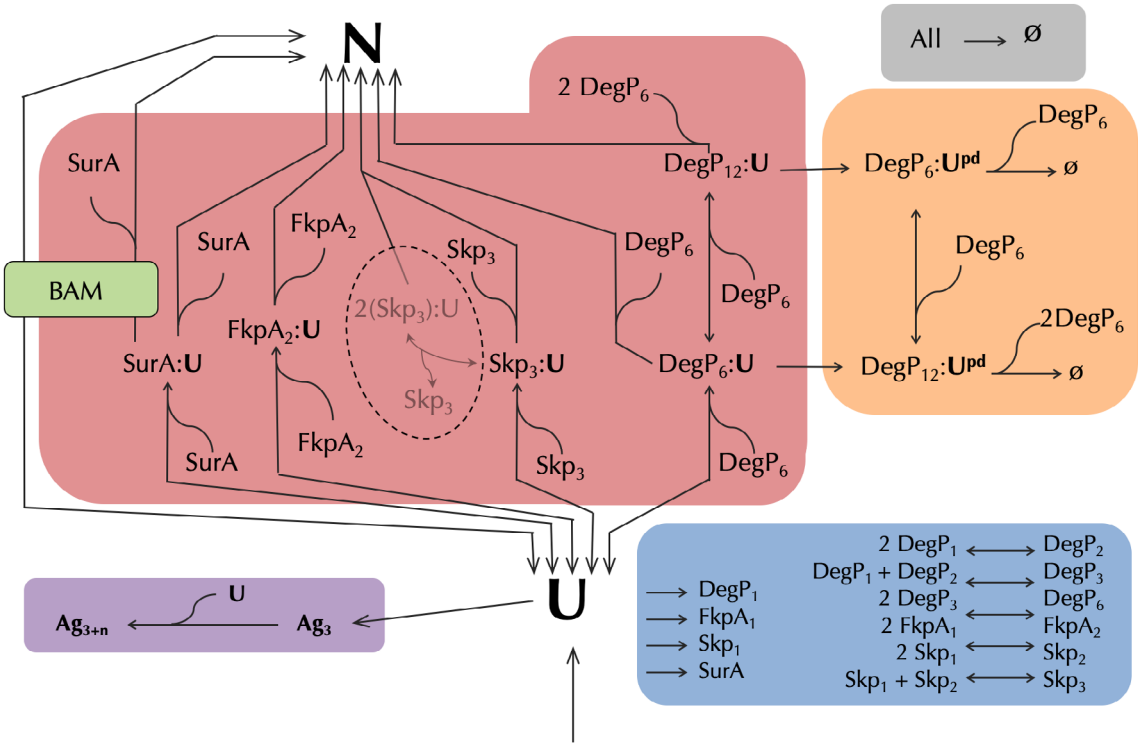

Figure 1. OMPBioM schematic. Schematic of the OMPBioM network model. This diagram was expanded from the basic model published in Costello,[15] where a detailed explanation is provided. The reactions inside the hashed oval circle are only included in the multivalency calculations as described in the text.

each genotype, we calculated 300 stochastic simulations each of duration 1000 s with a step size of 10^{-5} s. In addition to deleting reactions for the relevant genes in each null strain, parameters associated with the bacterial envelope stress response (σ^E) were incorporated into genetically observed null strains lacking SurA expression.[19] The σ^E stress response increases production of some chaperones and decreases OMP expression levels into the periplasm from the cytoplasm.[15,19,20] The final null strain employed was the nonbiologically observable Δ*surA** variant. This is a virtual strain lacking SurA calculated using wild-type parameters without the σ^E stress response. Outcomes from Δ*surA** are included because the results offer an opportunity to observe the species changes that lead to the induction of σ^E.

Figure 2 shows the observed population distributions for each null strain as indicated in the panel. The unbound uOMP, SurA:U, Skp_3:U, $FkpA_2$:U, and $DegP_{6/12}$:U (the sum of hexameric and dodecameric oligomers bound to uOMP) complexes are represented as a frequency of occurrence as a function of percentage occupancy in any particular trajectory from entry into the periplasm to folding. Figure 3 and Supporting Information Table S1 show the mean percentages from these distributions obtained from bootstrap analysis with replacement.

Figures 2 and 3 show that no single holdase:U species dominates for all of the null strain phenotypes. Instead, distinct chaperone complexes are enriched in different null strain phenotypes to achieve the same goal: to keep the free, unbound uOMP concentration depopulated. Under wild-type conditions, the $FkpA_2$:U species occupy the largest percentage of each trajectory with a mean percentage occupancy of 51%. This is significantly higher than that of the Skp_3:U species whose mean value is 29%. In Δ*skp*, the cell compensates for the loss of Skp expression by increasing the occupancy time of $FkpA_2$:U to 71%, a 140% increase over its value in the wild-type strain. Conversely, in Δ*fkpA*, the Skp_3:U occupancy doubles to 60% of the trajectory time to become the dominant chaperone complex. Together these findings indicate that Skp and FkpA are essentially interchangeable holdases.

What happens when the periplasm has neither FkpA nor Skp? Our results suggest that SurA moonlights as a holdase. In Δ*skp*Δ*fkpA*, the SurA:U mean occupancy time is 90%, which is a huge increase (500%) over its baseline percent occupancy in the wild-type strain (18%). SurA, therefore, is the *de facto* predominant holdase in Δ*skp*Δ*fkpA*. However, this finding should not be interpreted to appropriate a specialness to SurA holdase activity that is unveiled only when FkpA and Skp are both absent. In fact, the ability of SurA to fulfill the desired functional outcome of a holdase (e.g., low unbound uOMP) was there all along. Namely, the shift in SurA occupancy from a low level in the wild-type strain is less dramatic but still observable in both of the single null strains, for example, SurA:U occupancy doubles to 36% in Δ*fkpA* and rises to 26% in Δ*skp*. Importantly,

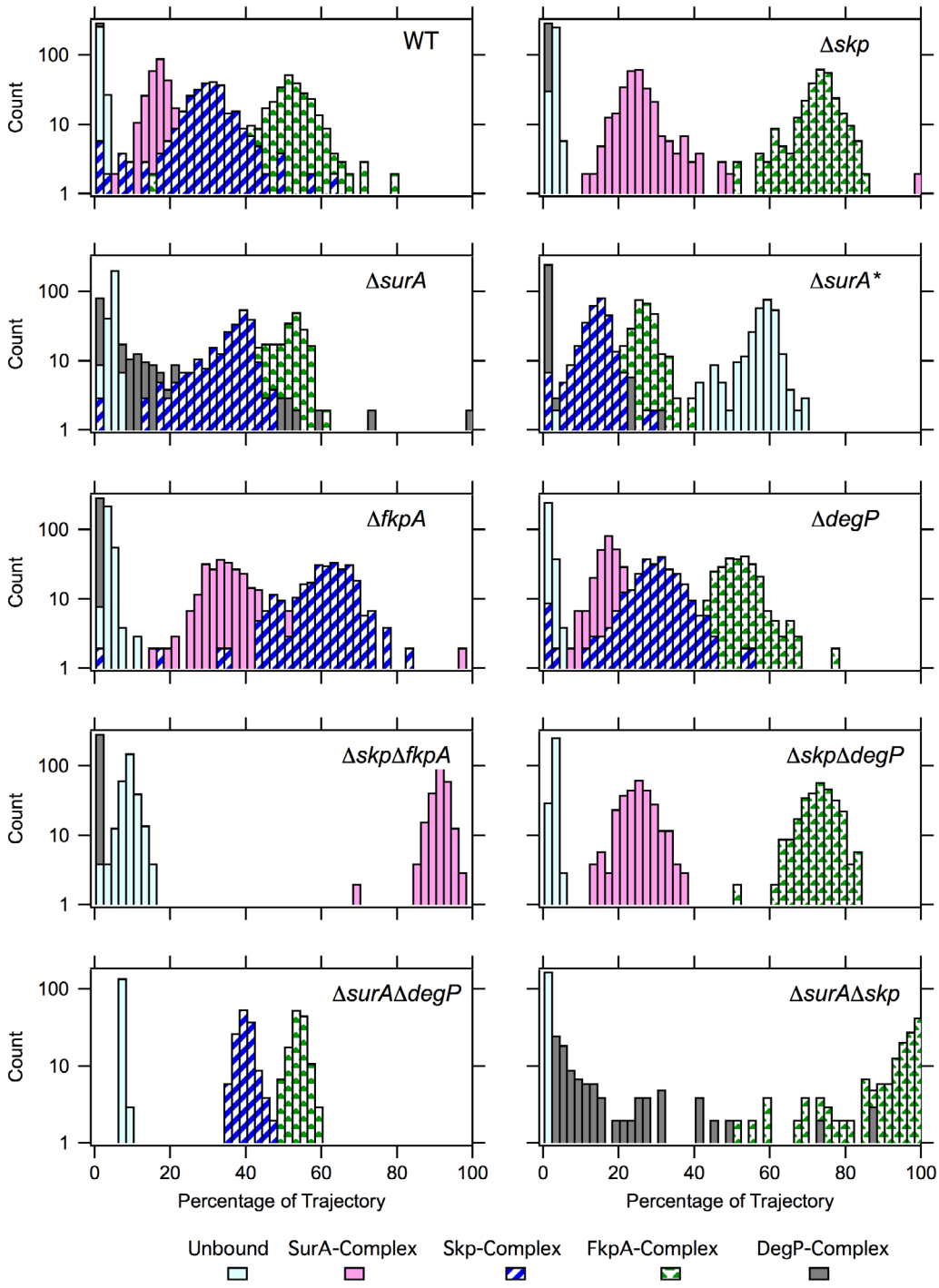

Figure 2. Distributions for chaperone–uOMP complex populations vary by genotype. The counts as a function of total percentage of time that a chaperone:uOMP complex exists during a trajectory are shown as a histogram distribution for all 300 simulations. Unbound is shown as light cyan; SurA:U complex is shown in solid pink bars; $FkpA_2$:U complex is shown in bars filled with green triangles; Skp_3:U complex is shown in bars with blue forward slash; and $DegP_{6/12}$:U complex is shown in gray-filled bars. Simulated strain identities are indicated in each panel.

these findings are not inconsistent with the accepted foldase function of SurA (Δ*surA*). Lack of SurA is a more detrimental phenotype as compared to either Δ*fkpA* or Δ*skp*,[15,21] consistent with the current understanding of SurA primarily as a foldase rather than a holdase. Moreover, SurA is the only chaperone of the set considered here to accelerate the folding of client uOMPs *in vitro*, and it shows a genetic interaction with the BAM complex.[8] These combined features result in the distinctive phenotypic response observed in Δ*surA* strains.

It is informative to use OMPBioM to consider how the various population distributions arise. The shifts in the chaperone–uOMP populations described

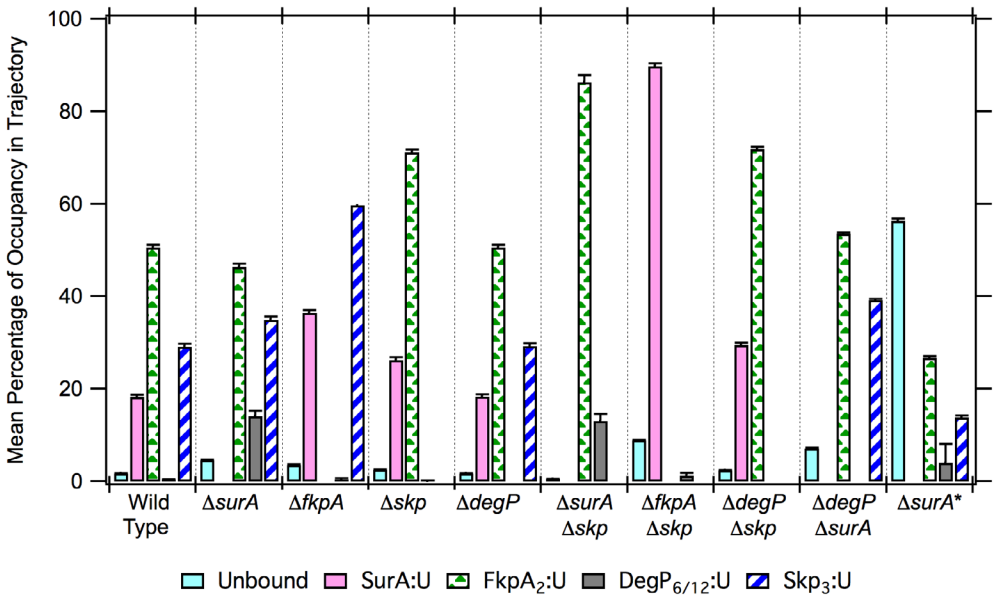

Figure 3. Mean values for chaperone–uOMP complex populations vary by genotype. Mean values for the distributions in Figure 2 were obtained by bootstrap methods and are plotted for each strain. Bar coloring is as described in Figure 2.

in the previous section are not a reflection of any changes in stability of any of the reactions. Particularly, in this computational model, it cannot be the case that either the forward or reverse rate constants or the affinity of any of the chaperones for an uOMP changes among Δ*fkp*A, Δskp, and Δ*fkp*AΔ*skp*. These values are predetermined inputs. Even in the stochastic simulations where an uncertainty is introduced on each rate constant, we previously observed that the lifetime distribution analyses of SurA:U, Skp_3:U, and $FkpA_2$:U complexes show that the best-fit dissociation rate constants correspond, as expected, to the deterministic rate constants (e.g., k_{19}, k_{21}, and k_{23} in Costello[15]). In contrast, the unbound uOMP lifetime is not predetermined. Instead, it is an emergent property of the collective action of all chaperones, their rate constants, and cellular expression levels. In this manner, the uOMP population and lifetime can vary depending on the components in the chaperone network. As an example, in the absence of the canonical holdases Skp and FkpA, a greater fraction of the unbound uOMP exists (compared to wild type[15]), which, through simple mass action, drives the increased population of the SurA:U complex.

Unbound, uOMP lifetimes are suppressed by the chaperone network

Holdases reduce self-aggregation of unfolded clients. Mass action formalism dictates that this suppression must be accomplished by binding to and stabilizing monomeric forms of clients. Therefore, holdases must compete with the intrinsic propensities of their clients to aggregate. Aggregation of unfolded OmpA (uOmpA) is characterized by a third-order nucleation step followed by an irreversible polymerization that all occur on the minutes time scale.[4,22] Thus, suppressing the formation of aggregate in this case means that the concentration of free uOMP must be kept at a low value. Our results suggest that the chaperone network accomplishes this by minimizing the unbound uOMP lifetime. Supporting Information Figure S1 shows that unbound uOMP lifetime distributions follow a single exponential distribution in all genotypes investigated, enabling best-fit values of the average lifetimes for each case. Indeed, these are short. In wild type, the unbound uOMP average lifetime is 0.0028 s, which is 30- to 125-fold shorter than any of the chaperone: uOMP complexes above. The absence of either Skp or FkpA increases the unbound uOMP lifetime to 0.0033 and 0.0059 s, respectively, which are still both much shorter than the lifetimes of the bound chaperone: uOMP complexes. The uOMP lifetime rises the most in null strains lacking SurA. The virtual Δ*surA** strain illustrates a hypothetical worst-case stress scenario for the cell, and the unbound uOMP lifetime rises 103-fold to 0.29 s. In the more realistic simulation of Δ*surA*, incorporating the σ^E stress response, the unbound uOMP lifetime drops to only fivefold above the wild-type value (to 0.012 s). Thus, suppressing the unbound uOMP lifetime, which is linked to its total concentration, is a defining feature of the network behavior.

Skp_3:U lifetimes cannot be on the same time scale as the E. coli *doubling time*

There is a wide disparity in the two reported lifetime measurements for Skp_3:U complexes. Zhao and colleagues used stopped-flow Förster resonance energy transfer to measure the dissociation of a Skp bound to unfolded OmpC (uOmpC) and found lifetimes in the millisecond range.[18] In contrast, Hiller and colleagues used nuclear magnetic resonance (NMR)

Table I. *Values Employed in Skp_3:U Lifetime Parameter Scan*

Simulation number	Lifetime (s)	k_{off} (s^{-1}) (k_{21})	K_D (nM)	k_{on} (M^{-1} s^{-1}) (k_{20})
1	9360 (2.6 h)	1.07E-4	16.4	6.54E3
2	936	1.07E-3	16.4	6.54E4
3	93.6	1.07E-2	16.4	6.54E5
4	9.36	1.07E-1	16.4	6.54E6
5	0.936	1.07	16.4	6.54E7
6	0.0936	0.107	16.4	6.54E8

The notations k_{20} and k_{21} refer to the rate constants governing the association and dissociation of Skp_3:U in Costello et al.[15]

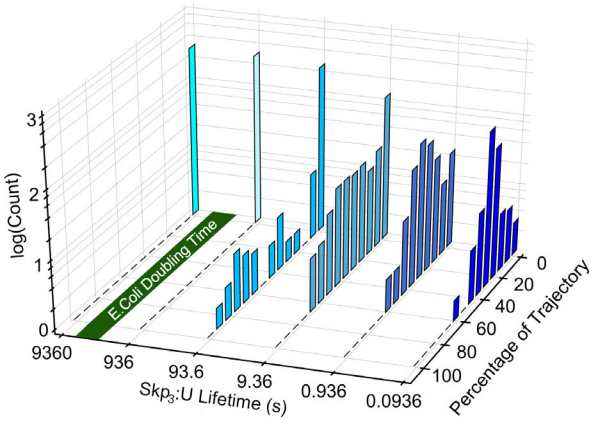

Figure 4. No Skp_3:U binding is observed when the complex lifetime is greater than the *E. coli* doubling time. Skp_3:U species percentage of trajectory distributions are shown for Skp_3:U lifetimes as indicated on the axis and using the values in Table I. No other chaperone parameters were modified in these simulations.

exchange and assumed off-rate-limited first-order kinetics to obtain a global lifetime constant of 2.6 ± 0.9 h for complex between Skp_3 and uOMP X (uOmpX).[17] Comparing the two values results in a ~30,000-fold difference between the two measurements, far beyond the expected uncertainty for each method. One possible reason for this discrepancy could be that the two investigations used unfolded clients that are quite different in size (~40 vs. ~16 kDa for OmpC and OmpX, respectively). A second explanation for the disagreement could arise from the fact that fluorescence and NMR techniques are conducted in different concentration regimes. However, total concentrations should not matter as long as the measured dissociation process was first order for both of these experiments, because the decay of the complex should be a single exponential function independent of protein concentration. In this case, the lifetime simply equals 1/*e* of the original signal. Exponential decays were shown for Zhao and colleagues, however, the bulk of the NMR exchange data were observed in the plateau region of that experiment. Despite the difference in the complex lifetimes, both these investigators as well as independent groups agree that the Skp_3:U complex's thermodynamic stability is characterized by an equilibrium dissociation constant in the nM range.[17,18,23,24]

To evaluate the possibility that distinct Skp_3:U complexes could indeed have very different lifetimes, we conducted six simulations in which we varied the lifetime (hence, the dissociation rate constant) for the Skp_3:U complex from hours to milliseconds. Table I provides values used in this parameter scan. Figure 4 shows the Skp_3:uOMP distributions over this range. The initially unexpected finding we observed was that no complex is formed if the lifetime is on the order of hours as illustrated by the single bar of zero percentage of the trajectory at 9360 s (2.6 h). Even if the lifetime is ~15 min (936 s), no Skp_3:U forms. Figure 5(A) shows the distributions of chaperone: uOMP species in which the Skp_3:U lifetime equals 2.6 h, where it can be observed that these distributions resemble those in the Δ*skp* strain in Figure 2 (top right panel). In both cases, the holdase role that Skp performs is carried out by FkpA and SurA. This paradox of "long lifetime - no binding" can be explained by the necessity to also set the on-rate constant for binding to a very slow value to satisfy the constraint for a nM dissociation constant. As a result, if the lifetime is on the time scale of minutes to hours, the bacteria double before Skp_3 even binds its uOMP client. Indeed, Figure 4 suggests that the Skp_3:U lifetime must be at least 10-fold shorter than the *E. coli* doubling time to appreciably populate Skp_3:U complexes. Only under conditions where this latter constraint is met does Skp becomes biologically relevant as a holdase. When this criterion is satisfied, OMPBioM does indicate that Skp_3:U complexes can have diverse lifetimes that range from the seconds to millisecond time scale.

A stoichiometry of two Skp trimers bound to one uOMP does not significantly change the chaperone distributions

Binding studies of Skp to small uOMPs has exhibited a stoichiometric complex formation consisting of one Skp trimer to one uOMP.[23,24] Subsequent to OMPBioM

Table II. *Reactions and Rate Constants Employed in the Multivalent Implementation of OMPBioM*

Reaction	Rate constant	Value	Units	Citations
uOMP : Skp_3 + Skp_3 → uOMP : 2(Skp_3)	k_{45}	1.75E+08	M^{-1} s^{-1}	Wu et al.[18]
uOMP : 2(Skp_3) → uOMP : Skp_3 + Skp_3	k_{46}	2.80E+00	s^{-1}	Wu et al.[18]
uOMP : 2(Skp_3) → fOMP + 2(Skp_3)	k_{47}	1.00E-09	s^{-1}	Patel et al.[34]

publication, Schiffrin et al. discovered using mass spectrometry that larger OMPs can simultaneously bind to two Skp trimers, forming a 2(Skp_3):U.[16] While no rate or equilibrium constants are available to directly describe the population of this multivalent species, we can incorporate it into OMPBioM by employing the same rate constants used to estimate the association and dissociation of the Skp_3:U complex. Accordingly, we conducted simulations using a network model that includes the reactions within the dashed oval in Figure 1. Table II details the rate constants for these reactions.

Figure 5(B) shows the mean population results from simulations that include the 2(Skp_3):U species. Figure 5(C,D) shows that the inclusion of the Skp multivalency results in modest effects on the overall chaperone population distributions as compared to the wild-type scenario (Fig. 2). To understand this finding, it is instructive to consider the outcome from both the perspective of uOMPs as well as Skp trimers. With respect to the uOMP client, the percentage of time a uOMP spends bound to Skp decreases when multivalency is included. Figure 5(B) shows that the mean percentages of occupancy in a trajectory in which a uOMP is bound to one or two Skp trimers equals 5% or 14%, respectively. This sums to a total percentage of 19%, which is lower than the mean percentage occupancy that a uOMP is bound to Skp in the original simulations (Fig. 2; wild type, 29%). The reduction in uOMP binding to Skp in the multivalent case can be rationalized by a lower concentration of free Skp trimer that is available to bind to a uOMP client. The formation of the multivalent 2(Skp_3):U species uses two Skp trimers for each complex formation and depletes the free Skp reactant population twice as much as compared to the formation of a Skp_3:U species. As a result of a lower free Skp trimer population, fewer Skp_3:U and 2(Skp_3):U species can be populated in the periplasm. From the perspective of number of Skp trimers bound to a uOMP, incorporating multivalency has little effect aside from shifting part of the Skp_3:U species into 2(Skp_3):U species. The absolute number of Skp trimers bound to uOMPs (Skp_{ToT}) is approximately the same as in the simulation without multivalency (29% vs. 33%), but these molecules are distributed across fewer complexes. Thus, from the perspective of Skp trimers binding to an uOMP, the multivalent reaction has no effect: the same number of Skp trimers are bound.

It is also interesting to consider how the remaining chaperone network reacts to Skp multivalency. Figure 5(B) shows that the minimal decrease in uOMPs bound to one or two Skp trimers is compensated by small increases in the percent of the lifetime that the uOMP spends bound to SurA or FkpA. OMPBioM could also formally consider additional multivalencies involving Skp; these species would

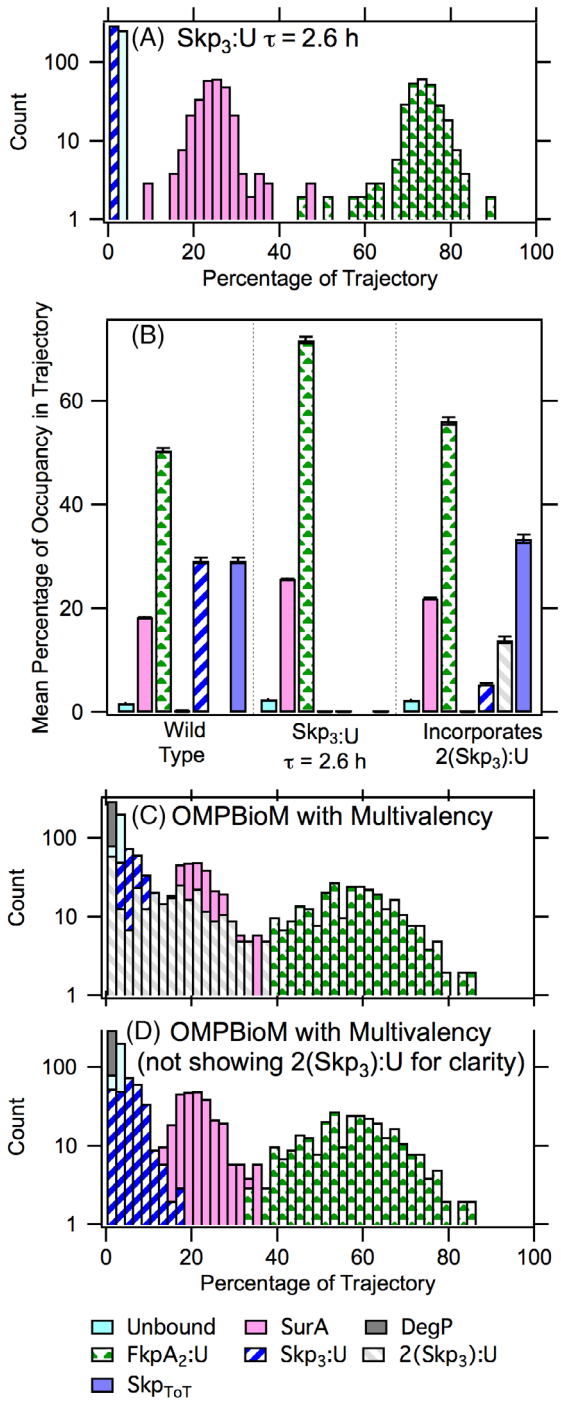

Figure 5. Chaperone complex distribution responses to parameter changes. Bar colors are shown as in Figure 2. (A) Species percentages of trajectory distributions are shown for all chaperone:uOMP complexes for the case where the Skp_3:U lifetime equals 2.6 h. (B) Mean values for the distributions shown in Figure 2 (WT, repeated here for direct comparison), with the addition of 2(Skp_3):U shown in bars with gray forward slash and summed total Skp in complex (in trimer units) in solid medium blue (far right bar). Values for these last two Skp forms are zero in the middle set of bars because the τ = 2.6 h simulation did not include the 2(Skp_3):U species; (C) Species percentages of trajectory distributions are shown for all chaperone:uOMP complexes for the case where Skp multivalency is included. (D) same data as in C except the 2(Skp_3):U distribution is not plotted in order to visualize (Skp_3):U.

deplete the Skp pool even more depending on the stoichiometry, and the actual number of complexes would decrease accordingly. In sum, the possibilities for multivalent chaperone-uOMP interactions further illustrates the redundancy within the periplasmic network and demonstrates the plasticity of the system.

Conclusions

Using OMPBioM to examine the distributions of Skp_3:U, 2(Skp_3):U, $FkpA_2$:U, and SurA:U complexes, we learn that the cell is agnostic to the details of the holdase activity as long as there is some threshold level of function. With the currently available data, mathematical modeling demonstrates that the concept of specific pathways is not an absolute requirement for functional robustness. Rather, the interconnected network structure articulated by OMPBioM illustrates how one holdase or another can meet the proteostasis needs of the cell. The network has steady state levels of occupancy of all species, but these are not static complexes with long lifetimes. Rather, functional redundancy is dynamically encoded through binding kinetics, thermodynamics, and local cellular concentrations, which serve to work together to tune the chaperone–uOMP interactions when no ATP or other external energy source is available. Interestingly, the cytoplasmic holdase trigger factor has a reported bound state lifetime of 100 ms, comparable to the chaperones discussed here, indicating fleeting interactions may be important even in environments containing external energy.[25] Overall, the mechanistic insight gained from OMPBioM is of particular interest because functionally redundant proteins are found across a wide range of biological systems ranging from yeast cells to astrocytes.[26–28] The fitness advantage of encoding redundancy is that it allows cells to respond more effectively to changing environments and to compensate for genetic mutations.[29] This adaptability is especially important for bacteria given their relatively short doubling times and their exposures to a wide range of extracellular conditions.

Methods

General

A full description of the model, including a list of reactions, parameters, and any relevant changes for the single- and double-null strain phenotypes, can be found in Costello et al.[15] Stochastic simulations of the wild-type model and the mutant strains were calculated with COPASI using the direct method.[30,31] Null strains were calculated by simple omission of the relevant reactions. In addition to null strains examined in the original report, we calculated values for a double null Δ*skp*Δ*fkpA*.

The simulation durations were 1000 s with an interval size of 10^{-5} s. We calculated 300 trajectories for each null strain. We analyzed outputs of these trajectories using MATLAB R2014a, where each individual lifetime of either the unbound OMP or a chaperone–OMP complex was calculated.

Unless otherwise indicated, the experiments here employed the rate constants published previously.[15] For Skp and SurA, the forward rate constants were calculated from the measured half times reported in Zhao and colleagues[18] using the following equation:

$$k = \frac{1}{t_{1/2}[A]_0}$$

This simplified equation applies because the reactant concentrations in those experiments were equal. Upon rechecking the calculations in response to a reviewer comment, we discovered that the value for the SurA forward rate constant was slightly larger than intended due to a transcription error (1.05×10^8 vs. 0.6×10^8). To demonstrate that this does not affect any of the results, we calculated 300 trajectories using the correct number, and this very small difference (less than twofold) has no effect on any of the distributions (Supporting Information Fig. S2). The forward rate constant for Skp was correct as reported.[15] The FkpA rate constants are based on the values reported.[9,15]

Chaperone complex lifetime calculations

Lifetimes were calculated for each of the six species of interest, for example, unbound uOMP, SurA:U, Skp_3:U, $FkpA_2$:U, and DegP:U. The lifetime for each occurrence is defined as the length of time in seconds of each continuous independent population of that species. The data for all 300 simulations were combined. A histogram plot describing the frequency of occurrence of each lifetime (for each species) was calculated using a bin size of 2 s. Binned counts were analyzed using a single exponential equation: $\text{Count}_t = \text{Count}_0 e^{-kt}$, where Count_t and Count_0 equal the occurrence number at times $t = t_i$ and $t = 0$ and k = the rate constant (s^{-1}). The excellent fit to this equation confirms the expected first-order behavior for the lifetime, τ (s), which is the inverse of the rate constant.

Chaperone complex percentage calculations

The total percentage of time during a trajectory for each of the six species was calculated by summing the total time of occurrence for a species in a trajectory divided the trajectory time, where the trajectory time is defined here as the time it takes for a uOMP to fold in that trajectory. These percentage values were calculated for each of the 300 simulations and combined for each species. The distribution plot describing the distributions of percentage values (for

each species) was calculated using a bin size of 2%. The mean percentages for each species was obtained by bootstrapping with replacement using the MATLAB bootstrapping function.[32] To ensure convergence[33] and to obtain 90% confidence intervals, we set the number of bootstrap resamples to 5, 10, 50, 100, 500, 1000, 5000, and 10,000. The lifetimes were summed to determine the percentage of each trajectory spent in each state. In several strains, a small number of trajectories did not end in either a folded or degraded state after 1000 s. These incomplete trajectories were eliminated from the subsequent analysis to prevent interrupted complexes from skewing the average lifetimes.

Skp3:U lifetime parameter scan

Six lifetime parameter scans were calculated using COPASI with the direct method (Gillespie).[30,31] The substituted parameters are indicated for each simulation in Table I. We calculated 300 trajectories for each condition and analyzed these outputs as described above.

Incorporation of multivalency: calculations of the 2(Skp_3):U complex

The formation of 2(Skp_3):U was added to OMPBioM by incorporating the reactions in Table II into the existing wild-type model. In the absence of direct measurements for the binding constants for these new reactions, we assumed an identical independent binding scenario and used the same rate constant values that characterize the association and dissociation the Skp_3:U species.

Acknowledgments

This research project was conducted using computational resources at the Maryland Advanced Research Computing Center. The authors thank lab members for helpful discussions.

References

1. Fernandez-Funez P, Sanchez-Garcia J, de Mena L, Zhang Y, Levites Y, Khare S, Golde TE, Rincon-Limas DE (2016) Holdase activity of secreted Hsp70 masks amyloid-β42 neurotoxicity in *Drosophila*. Proc Natl Acad Sci U S A 113:E5212–E5221.
2. Hoffmann JH, Linke K, Graf PC, Lilie H, Jakob U (2004) Identification of a redox-regulated chaperone network. EMBO J 23:160–168.
3. Beissinger M, Buchner J (1998) How chaperones fold proteins. Biol Chem 379:245–259.
4. Danoff EJ, Fleming KG (2015) Aqueous, unfolded OmpA forms amyloid-like fibrils upon self-association. PLoS One 10:e0132301.
5. Ebie Tan A, Burgess NK, DeAndrade DS, Marold JD, Fleming KG (2010) Self-association of unfolded outer membrane proteins. Macromol Biosci 10:763–767.
6. Walton TA, Sousa MC (2004) Crystal structure of Skp, a prefoldin-like chaperone that protects soluble and membrane proteins from aggregation. Mol Cell 15:367–374.
7. Walton TA, Sandoval CM, Fowler CA, Pardi A, Sousa MC (2009) The cavity-chaperone Skp protects its substrate from aggregation but allows independent folding of substrate domains. Proc Natl Acad Sci U S A 106: 1772–1777.
8. Sklar JG, Wu T, Kahne D, Silhavy TJ (2007) Defining the roles of the periplasmic chaperones SurA, Skp, and DegP in *Escherichia coli*. Genes Dev 21:2473–2484.
9. Ge X, Lyu Z-X, Liu Y, Wang R, Zhao XS, Fu X, Chang Z (2014) Identification of FkpA as a key quality control factor for the biogenesis of outer membrane proteins under heat shock conditions. J Bacteriol 196:672–680.
10. Chen R, Henning U (1996) A periplasmic protein (Skp) of *Escherichia coli* selectively binds a class of outer membrane proteins. Mol Microbiol 19:1287–1294.
11. Behrens S, Maier R, De Cock H, Schmid FX, Gross CA (2001) The SurA periplasmic PPIase lacking its parvulin domains functions in vivo and has chaperone activity. EMBO J 20:285–294.
12. Lazar SW, Kolter R (1996) SurA assists the folding of *Escherichia coli* outer membrane proteins. J Bacteriol 178:1770–1773.
13. Ge X, Wang R, Ma J, Liu Y, Ezemaduka AN, Chen PR, Fu X, Chang Z (2014) DegP primarily functions as a protease for the biogenesis of beta-barrel outer membrane proteins in the Gram-negative bacterium *Escherichia coli*. FEBS J 281:1226–1240.
14. Rizzitello AE, Harper JR, Silhavy TJ (2001) Genetic evidence for parallel pathways of chaperone activity in the periplasm of *Escherichia coli*. J Bacteriol 183:6794–6800.
15. Costello SM, Plummer AM, Fleming PJ, Fleming KG (2016) Dynamic periplasmic chaperone reservoir facilitates biogenesis of outer membrane proteins. Proc Natl Acad Sci U S A 113:E4794–E4800.
16. Schiffrin B, Calabrese AN, Devine PWA, Harris SA, Ashcroft AE, Brockwell DJ, Radford SE (2016) Skp is a multivalent chaperone of outer-membrane proteins. Nat Struct Mol Biol 23:786–793.
17. Burmann BM, Wang C, Hiller S (2013) Conformation and dynamics of the periplasmic membrane-protein-chaperone complexes OmpX-Skp and tOmpA-Skp. Nat Struct Mol Biol 20:1265–1272.
18. Wu S, Ge X, Lv Z, Zhi Z, Chang Z, Zhao XS (2011) Interaction between bacterial outer membrane proteins and periplasmic quality control factors: a kinetic partitioning mechanism. Biochem J 438:505–511.
19. Mecsas J, Rouviere PE, Erickson JW, Donohue TJ, Gross CA (1993) The activity of sigma E, an *Escherichia coli* heat-inducible sigma-factor, is modulated by expression of outer membrane proteins. Genes Dev 7:2618–2628.
20. Dartigalongue C, Missiakas D, Raina S (2001) Characterization of the *Escherichia coli* sigma E regulon. J Biol Chem 276:20866–20875.
21. Rouviere PE, Gross CA (1996) SurA, a periplasmic protein with peptidyl-prolyl isomerase activity, participates in the assembly of outer membrane porins. Genes Dev 10:3170–3182.
22. Danoff EJ, Fleming KG (2011) The soluble, periplasmic domain of OmpA folds as an independent unit and displays chaperone activity by reducing the self-association propensity of the unfolded OmpA transmembrane beta-barrel. Biophys Chem 159:194–204.
23. Qu J, Mayer C, Behrens S, Holst O, Kleinschmidt JH (2007) The trimeric periplasmic chaperone Skp of *Escherichia coli* forms 1:1 complexes with outer membrane proteins via hydrophobic and electrostatic interactions. J Mol Biol 374:91–105.
24. Moon CP, Zaccai NR, Fleming PJ, Gessman D, Fleming KG (2013) Membrane protein stability may be

the energy sink for sorting in the periplasm. Proc Natl Acad Sci U S A 110:5285–5290.
25. Maier R, Scholz C, Schmid FX (2001) Dynamic association of trigger factor with protein substrates. J Mol Biol 314:1181–1190.
26. Dean EJ, Davis JC, Davis RW, Petrov DA (2008) Pervasive and persistent redundancy among duplicated genes in yeast. PLoS Genet 4:e1000113.
27. Nowak MA, Boerlijst MC, Cooke J, Smith JM (1997) Evolution of genetic redundancy. Nature 388:167–171.
28. Pekny M, Levéen P, Pekna M, Eliasson C, Berthold CH, Westermark B, Betsholtz C (1995) Mice lacking glial fibrillary acidic protein display astrocytes devoid of intermediate filaments but develop and reproduce normally. EMBO J 14:1590–1598.
29. Kafri R, Springer M, Pilpel Y (2009) Genetic redundancy: new tricks for old genes. Cell 136:389–392.
30. Gillespie DT (1976) A general method for numerically simulating the stochastic time evolution of coupled chemical reactions. J Comput Phys 22:403–434.
31. Hoops S, Sahle S, Gauges R, Lee C, Pahle J, Simus N, Singhal M, Xu L, Mendes P, Kummer U (2006) COPASI–a COmplex PAthway SImulator. Bioinformatics 22:3067–3074.
32. Efron B (1979) 1977 Rietz lecture—bootstrap methods—another look at the jackknife. Ann Stat 7:1–26.
33. Carpenter J, Bithell J (2000) Bootstrap confidence intervals: when, which, what? A practical guide for medical statisticians. Stat Med 19:1141–1164.
34. Patel GJ, Behrens-Kneip S, Holst O, Kleinschmidt JH (2009) The periplasmic chaperone Skp facilitates targeting, insertion, and folding of OmpA into lipid membranes with a negative membrane surface potential. Biochemistry 48:10235–10245.